Finite Element Modeling of Reinforced Concrete Beam Patch Repaired and Strengthened with Fiber-Reinforced Polymers

Mundeli Salathiel , Mbereyaho Leopold , Pilate MOYO

Abstract— **Repair and strengthening using Fiber Reinforced Polymers (FRP) have been one of worldwide methods used to improve the load carrying capacity and durability of reinforced concrete structural elements such as beams, in decline mainly due to corrosion of steel reinforcement resulting from the deterioration of the concrete cover. The main objective of this study was to investigate the behavior of reinforced concrete beam patch repaired and strengthened with FRP composites. The 3D finite element analysis was conducted using Abaqus software, while the repair consisted of varying the length of the patch, where four patch lengths were considered. Isotropic concrete damaged plasticity model was applied to describe the behavior of both concrete and repair material. Linear elastic-perfectly plastic and linear elastic isotropic model were used for steel and FRP; respectively, while cohesive bond model was used for the interface between concrete and FRP. Numerical results show good agreement with experimental findings in terms of load-deflection curves, crack pattern and modes of failure. The study also revealed that for proper structural crack distribution, it is better to use force control while for failure mechanism, displacement control is the best choice. Finally, once again it was proved that both patch repair and FRP strengthening increased the load carrying capacity and affected crack distribution.**

Index Terms — **cracking, constitutive model, damage, debonding, Fiber Reinforced Polymers (FRP), finite elements, prediction, repair, strengthening.**

I. INTRODUCTION

Reinforced concrete structural elements such as beams get deteriorated and become structurally and functionally inadequate, due to corrosion of steel reinforcement resulting from concrete cracking and spalling, poor design and maintenance and natural disasters such as earthquake. To upgrade the load carrying capacity and durability of such concrete elements, repair and structural strengthening have been used all over the world since last decades. While repair consists of removing damaged concrete, preparation of concrete substrate and application of a new layer of repair material, strengthening consists of bonding a steel plate or a fiber reinforced polymer (FRP) plate to the tension face of the

beam. FRP composites have been extensively used due to their advantages over steel plates such as corrosion resistance, lightweight and high strength. FRP plates are bonded to concrete substrate by means of adhesive.

Such patch repaired and FRP-strengthened beams may fail in a similar way to that of unstrengthened reinforced concrete beams but quite often they fail by debonding in two modes [25]: (1) Intermediate crack induced debonding which initiates around critical flexural cracks and propagates towards the plate end, and (2) plate end debonding initiating at the plate end due to high stress concentration and critical shear cracks (Figure 1). Thus, debonding is speeded up by crack propagation particularly in the horizontal direction [25]. Cracks may also form in different locations in the interface between concrete and FRP and may cause the failure of the interface inside the adhesive, at the interface between adhesive and concrete or at the interface between adhesive and FRP, inside the FRP or within the concrete cover [6].
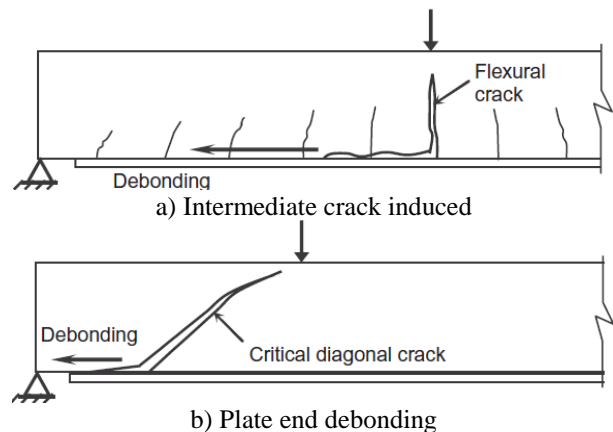

a) Intermediate crack induced

b) Plate end debonding
Figure1. Debonding failure modes

Among the failure modes of reinforced concrete strengthened beams, debonding is quite difficult to predict. In fact, crushing strain of concrete is known, yielding of tension steel can be measured in the laboratory and hence predicted and FRP rupture can be predicted from rupture strain provided by the manufacturer; but debonding control is still not well understood.

Different approaches have been used to predict the behavior of such beams and include analytical [14, 22, 24, 26], experimental [14, 15, 18, 20], numerical [4, 8, 23] and fracture mechanics [3, 10, 19]. However, such approaches face some limitations due to complex behavior of concrete and that of the interface between concrete and FRP. Such complexity for concrete is due to the nonlinear load-deformation response of concrete and difficulty in forming suitable constitutive relationships under combined stresses, progressive cracking of concrete under increasing load and the complexity in the formulation of the failure

Mr Mundeli Salathiel, Department of Civil, Environmental and Geomatic Engineering (CEGE), School of Engineering, College of Science and Technology (CST), University of Rwanda (UR) , Kigali City, Rwanda. Mobile Phone No: + 250788864091.
Dr Mbereyaho Leopold, Department of Civil, Environmental and Geomatic Engineering (CEGE), School of Engineering, College of Science and Technology (CST), University of Rwanda (UR), Kigali City, Rwanda., Mobile Phone No: + 250788474046.
Prof. Pilate MOYO, University of Cape Town, Department of Civil Engineering, Rondebosch, Western Cape, South Africa. Mobile Phone No:+27721053366.

behavior for various stress states, the consideration of steel and its interaction with concrete and time dependent effects such as creep and shrinkage of concrete [5].

Even though such approaches have been used for studying the behavior and failure mechanisms of patch repaired and FRP-strengthened RC beams, no numerical study using finite elements method has been done so far taking into consideration the effect of patch repair. The finite element method application requires a good understanding of the mechanical behavior of various materials involved, thus the requirements of constitutive relationships for the description of such behavior.

This paper presents a finite element analysis of patch repaired and FRP-strengthened RC beams with varying patch length and loaded in four points bending. Their behavior in terms of load-displacement response, crack pattern, failure mechanisms and strain distribution in FRP is studied and validation against experimental results obtained from the same beams is done.

II. FINITE ELEMENT MODELING

The finite element analysis performed in this study consisted of modeling the nonlinear behavior of reinforced concrete beams patch repaired and strengthened with FRP bonded to their tension face to investigate the behavior of such RC beams under four points bending. The commercial finite element package ABAQUS software was used. The beam modeled in 3D is shown in Figure 2. The beam was reinforced with 2Y20 in tension and 2Y8 in compression. Shear reinforcement consisted of 8mm diameter stirrups at 80mm c/c distributed equally over the whole length of the beam as shown in Figure 2. The FRP reinforcement was placed at a distance of 50mm from the support. While the height of the patch repair was maintained at 105mm, the length was varied as 450, 800, 1300 and 1800mm.
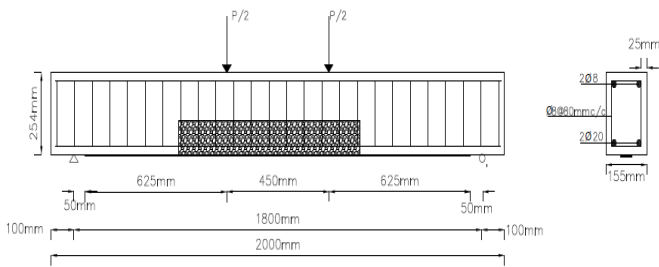
.

Figure 2. Geometry, reinforcement and FRP setup of the beam (800mm patch length)

2.1. Material properties and constitutive models
2.1.1. Concrete

There are three models available in Abaqus for the analysis of concrete at low confining pressure: Concrete smeared cracking model in Abaqus/Standard, Brittle cracking model in Abaqus/Explicit and Concrete damaged plasticity model in Abaqus/Standard and Abaqus Explicit. Concrete undergoes both inelastic deformation and stiffness degradation when loaded. However, those two are not captured at the same time by concrete smeared crack model and brittle cracking model. In concrete smeared crack model, cracking is the most important aspect of the behavior and a compression yield

surface is used to control plastic straining in compression whereas in brittle cracking model compressive failure is not important [1]. Concrete damaged plasticity; available in ABAQUS; due to its capability of capturing both inelastic deformation and stiffness degradation, was used in this study. The compressive strength was experimentally determined at the age of 28 days as 50MPa and 70MPa for concrete and repair material, respectively. The elastic parameters necessary for the establishment of the first part of the model were the secant modulus of elasticity E_{cm} and mean axial tensile strength, f_{ctm} and were calculated according to [9] as:

$$E_{cm} = 22[(f_{cm})/10]^{0.3} = 35000 MPa \qquad (1)$$

$$f_{ctm} = 0.30(f_{ck})^{(2/3)} = 3.5 Mpa \qquad (2)$$

For concrete

$$E_{cm} = 22[(f_{cm})/10]^{0.3} = 38400 MPa \qquad (3)$$

$$f_{ctm} = 2.12\ln[1 + (f_{cm}/10)] = 4.3 Mpa \qquad (4)$$

For repair material, the post-peak behavior in tension was represented with tension stiffening to simulate the effects of concrete/steel effects such as bond slip and dowel action. Tension stiffening was specified in terms of fracture energy criterion. A fracture energy of $0.08 N/mm$ and $0.15 N/mm$ were used for concrete and repair material, respectively. The tensile stress in concrete was reduced to zero at a tensile strain of 0.001 for both concrete and repair material [1]. The nonlinear uniaxial compression stress-strain curve was constructed based on the expression proposed by [9]:
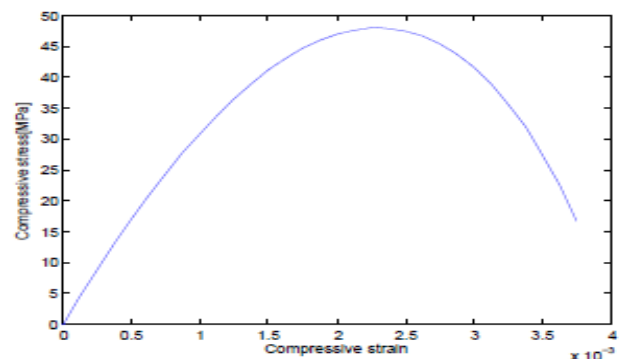
$$\frac{\sigma_c}{f_{cm}} = \frac{k\eta - \eta^2}{1 + (k-2)} \qquad (4)$$

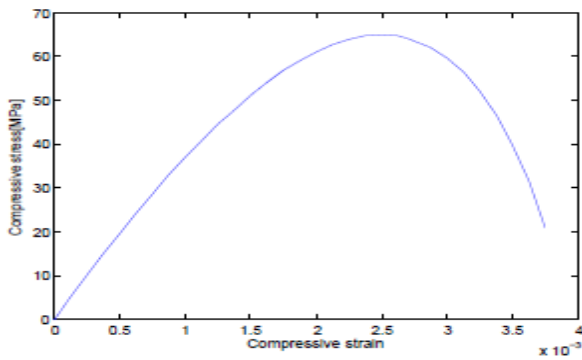$$\eta = \frac{\varepsilon_c}{\varepsilon_{c1}} \qquad k = 1.05\frac{|\varepsilon_{c1}|}{f_{cm}}$$

Where and

$\varepsilon_{c1} = 0.7 f_{cm}^{0.31} \leq 2.8$ ‰, f_{cm} is the mean value of concrete cylinder compressive strength derived from concrete cube strength and σ_c is the compressive stress in concrete. The curve is shown in Figure 3 for both concrete and repair material.

(a)

(b)

Figure3. Uniaxial compressive behavior:
(a) Concrete, (b) Repair material

The cracking strain and inelastic strain for both concrete and repair material were determined by taking the total strain minus the elastic strain corresponding to the undamaged material. On the other hand, concrete tension and compression damage were defined through tensile and compressive damage parameters defined as :

$$D_{c,t} = 1 - \frac{f_{c,t}}{\sigma_{c,t}} \quad (5)$$

Where D is the damage parameter equal to zero for undamaged material and one for a completely damaged material, f is the stress on the descending branch on the uniaxial stress strain curve, σ is the ultimate stress and the subscripts c and t stand for compression and tension, respectively. For plasticity parameters, except the dilatation angle that was taken as 370, other parameters were assigned default values as suggested by [1].

The criterion for concrete cracking under tension was defined in terms of maximum principal stress, which was taken equal to tensile strength of concrete. Since crack propagation requires energy consumption, the energy required to open a unit area crack, Gf as defined by [11] was used. The same philosophy was also applied to repair material.

2.1.2. Steel reinforcement
Since the properties of steel do not depend on environmental conditions or time, steel exhibits the same stress-strain curve in compression and in tension [12]. Tension, compression and shear reinforcements were assumed to behave in an elastic perfectly plastic manner in both compression and tension as shown in figure 4. The modulus of elasticity of steel was taken as 200 GPa while the yield stress was taken as 460MPa for longitudinal reinforcement and 250MPa for shear reinforcement. Poisson's ratio was taken as 0.3.
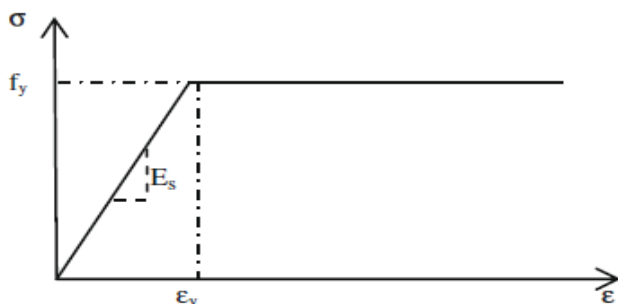

Figure4. Behavior of steel in tension and compression

Tension reinforcements were partitioned and their cross sections were reduced by 10% over a length equal to that of the repair to simulate the corrosion effects since corrosion results in steel cross section reduction and hence mass loss.

2.1.3. Fiber Reinforced Polymers Material
Fiber Reinforced Polymers are made of high strength fibers of glass, aramid or carbon embedded in a polymer resin called matrix. Fibers may be arranged so that they are oriented in directions of high stresses (anisotropic) or are oriented only in one direction (isotropic). FRP material behaves in a linear elastic manner up to failure. For flexural strengthening, the elastic modulus in fiber direction is of most importance. Therefore, in this study the isotropic elastic type was used for characterization of mechanical properties of Carbon Fiber Reinforced Polymer (CFRP) since they were unidirectional with high stiffness. The elastic modulus in fiber direction was specified by the manufacturer as 165GPa and the Poisson's ratio was taken as 0.3. The minimum value of strain at break in fiber direction was given by the manufacturer as 1.70%. The width of the CFRP used was 50mm with a thickness of 1.2mm. This thickness was reserved in order to facilitate the installation of warp fabrics at the plate end to prevent early end plate debonding. Only one layer of CFRP used was bonded to concrete by means of adhesive epoxy. The adhesive layer constituted the interface between concrete and CFRP material.

2.1.4. Adhesive-Concrete/CFRP interface.
The interface between concrete and FRP is critical in FRP-strengthened RC beams. It ensures the transfer of both shear and normal stresses from concrete to FRP as it resists their separation. The layer of adhesive between concrete and FRP of 1mm thickness was modeled using cohesive zone model. The model is characterized by a progressive stiffness degradation driven by a damage process. Cohesive zone model used in this study is graphically represented by a simple bilinear traction separation law, i.e. linear elastic traction shown in figure 5.
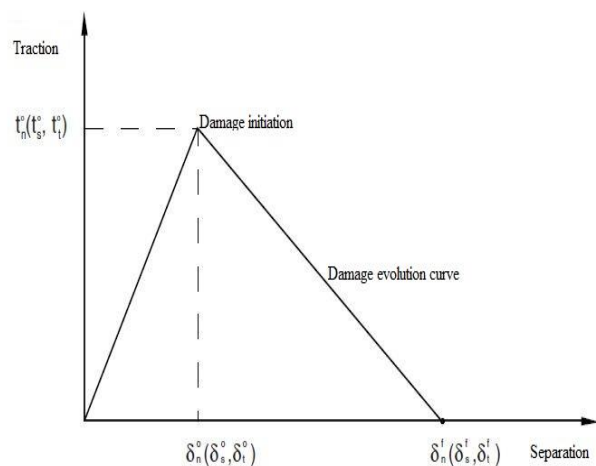

Figure 5. Bilinear traction separation law

It was accepted that the interface was subjected to normal stress and shear stress in two shear directions. The initiation of damage was assumed to take place when the maximum nominal stress ratios reached a value of one [1].

$$\max\left\{\frac{\langle t_n \rangle}{t_n^0}, \frac{t_s}{t_s^0}, \frac{t_t}{t_t^0}\right\} = 1$$

(6)

where t_n^0, t_s^0 and t_t^0 represent the peak values of the nominal stress when the deformation is either purely in normal or purely in the first or second shear directions.

The values used in this study were $t_n^0 = 4MPa$ and $t_s^0 = t_t^0 = 15MPa$ according to the manufacturer. Since the thickness of the adhesive layer was one mm, the ratio of elastic modulus and normal stiffness, shear modulus and shear stiffness were taken equal to one. Damage evolution was defined in terms of displacement at failure.

III. METHODOLOGY FOR THE STUDY

In this study, different parts making up the complete model were created in Abaqus/Standard in 3D modeling space. To ensure a perfect bond between concrete and repair material; concrete and adhesive; concrete beam was portioned to the size of the adhesive and different length of repair material. The thickness of the adhesive was 1mm.

Two-node linear 3D (T3D2) truss elements were used for longitudinal and shear reinforcements. The interface between concrete and CFRP was modeled using 8-node three-dimensional cohesive elements (COH3D8). Eight-node linear brick elements were used for concrete, repair material and CFRP. Different element shapes adopted in this study are shown in Figure 6. Three meshing techniques were used: structured meshing technique for concrete repair material and CFRP; swept meshing technique for the adhesive and free meshing technique for steel. Figure 6 shows a typical mesh (made coarser for clarity) for reinforced concrete beam with 800mm patch strengthened with CFRP.
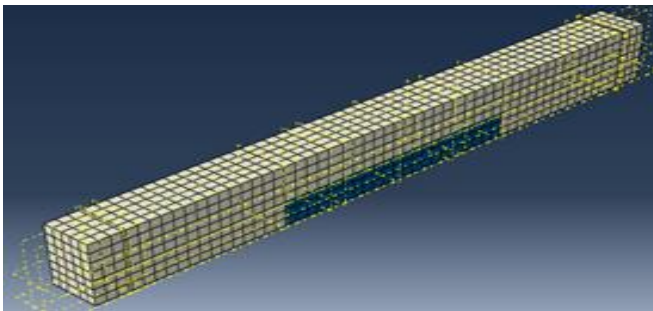

Figure 6. Finite element model for patch-repaired and CFRP strengthened RC beam (800mm-Patch) [17]

The perfect bond model between concrete and steel was adopted. It was implemented by embedding steel reinforcement in concrete, i.e. incorporation of one dimensional element into a three dimensional elements allowing reinforcing bars to pass through concrete elements in an arbitrary fashion [21] thus, introducing new nodes in the concrete elements. Full Newton solution technique was used in this analysis. In this method, the solution to nonlinear problems is obtained by defining the load as a function of time and breaking the simulation into a number of time increments and finds the approximate equilibrium at the end of each time

increment [11]. Thus, the issue was to choose the initial increment size. In this study, the initial increment size was 10% of the total step time.

IV. RESULTS AND DISCUSSIONS

As stated earlier, the main objective of this study was to investigate the behavior of reinforced concrete beams patch repaired and strengthened with FRP composites. The parameter that was varied was the length of the patch by keeping constant its depth. Such behavior was studied in terms of crack initiation and propagation, load-deflection relationships, damage energy release rate, failure mechanisms and strain distribution in the FRP for strengthened beams only.

For validation purpose, a comparison with experimental results obtained from the same beams is done. This section presents the results obtained from finite elements analysis for the above parameters.

4.1. Cracking initiation and evolution

Cracking was initiated whenever the maximum principal stress was greater than the tensile strength of concrete which was 3.5 MPa for concrete and 4.3MPa for repair material. This may be seen from Figure 7, which shows the distribution of tensile stresses for control beam where the maximum averaged tensile stress was 3.7MPa for concrete but not averaged value was 3.6MPa which was always greater than tensile strength. This value was found after the first increment. For patch-repaired RC beams, for example 1800mm-Patch, an averaged tensile stress of 4.4MPa was found at the third increment. At the same time, not averaged tensile stress of 4.4 was probed in the bottom center. This value is greater than the tensile strength of the repair material and this involves cracking since tensile strength was exceeded.
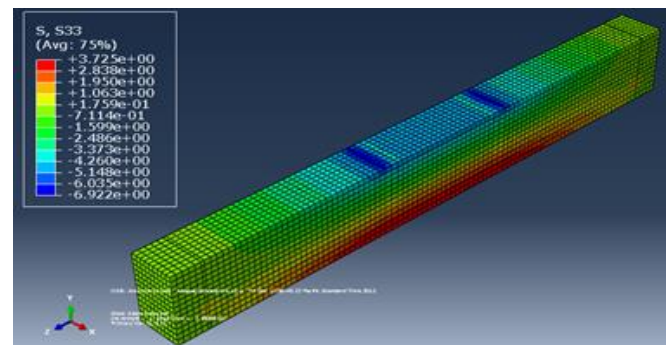

Figure 7. Cracking initiation for control beam [17]

Even if cracking for control beam took place after the first increment, the cracking load was found to be higher than that of patch repaired and strengthened beams though for such beams it took place after the third increment for 450mm, 800mm and 1800mm patched beams and after the fourth increment for 1300mm patch repaired beam. For patch-repaired and strengthened beams cracking loads were lower as compared to control beam. Figure 8 compares cracking loads from both experiments and finite elements analysis while Figure 9 compares structural crack pattern for control beam and 1800mm patched beam. For graphical visualization of cracks using concrete damaged plasticity

model for concrete and repair material, it was assumed that cracking initiated at points where the tensile equivalent plastic strain was greater than zero and the maximum principal plastic strain was positive [13]. It is important to note that in this study no precracking was considered. Force control was used for structural crack distribution.
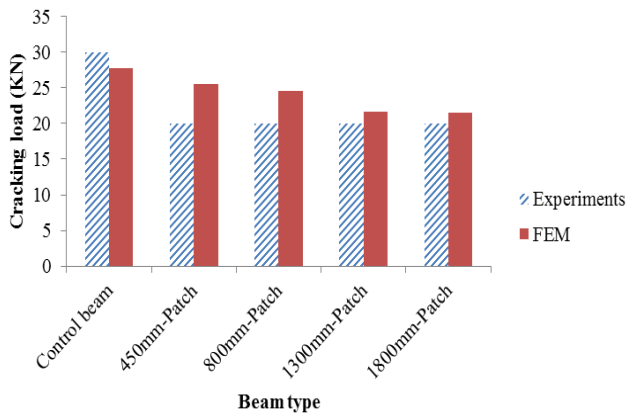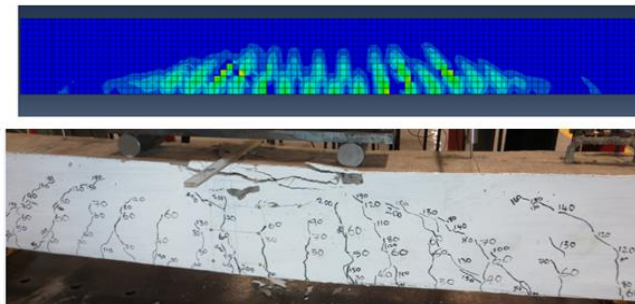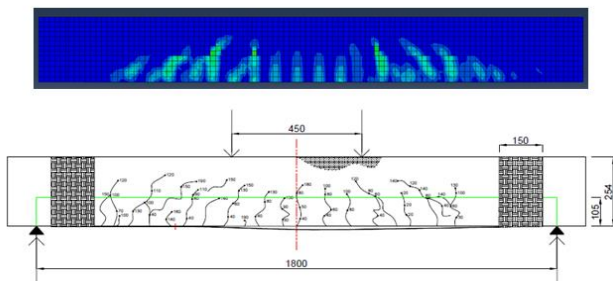

Figure 8: Cracking loads [17]

(a) Control beam

(b) 1800mm patched beam
Figure 9: Structural crack pattern

4.2. Load deflection relationships.

Generally, the behavior of reinforced concrete beams subjected to bending is analyzed through load-deflection curves. Mid-span load-deflection relationships represent failure stages as the applied load increases. Those stages include cracking initiation, yielding of steel reinforcement, debonding loads for strengthened beams and ultimate load. Load deflection curves obtained from control beam and four patch repaired and strengthened beams are shown in Figure 10 in comparison to experimental results. As it can be seen, there is a close agreement between numerical results and experimental findings. This clearly, shows the ability of the proposed model for analyzing the overall behavior of patch-repaired beams and strengthened with FRP composites. There are however, some differences between numerical and experimental results, which were due to the assumptions made in the finite elements formulation and the fact that beams were

not anchored as in experiment. In addition, as reported by [7], concrete damaged plasticity overestimates the stresses in concrete and this could also be a reason of discrepancies. It is observed that for control RC beam after yielding of steel no further increment in load carrying capacity was experienced until failure. However, for patch repaired and FRP strengthened beams, this was not the case. This shows that repair and strengthening increase the load carrying capacity of reinforced concrete beams in addition to increasing their service life.
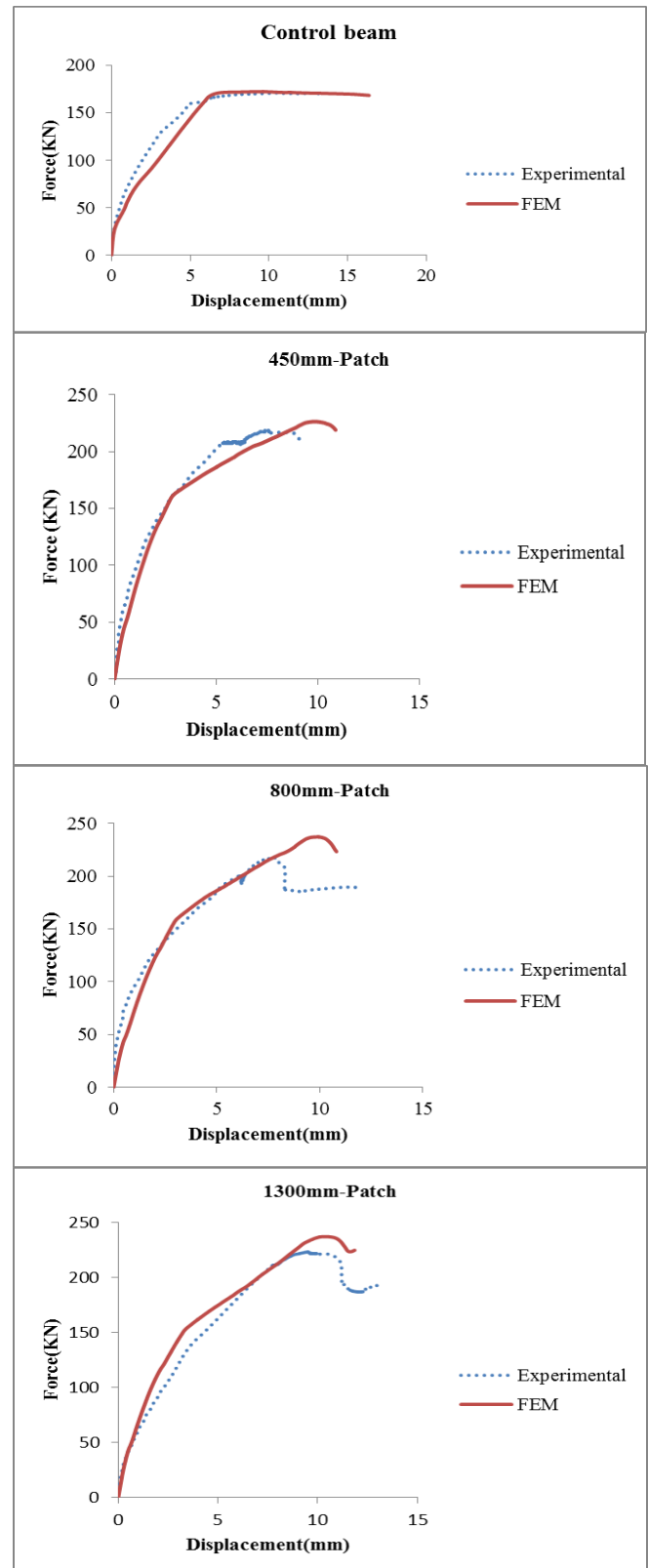
Figure 12. Damage energy release rates
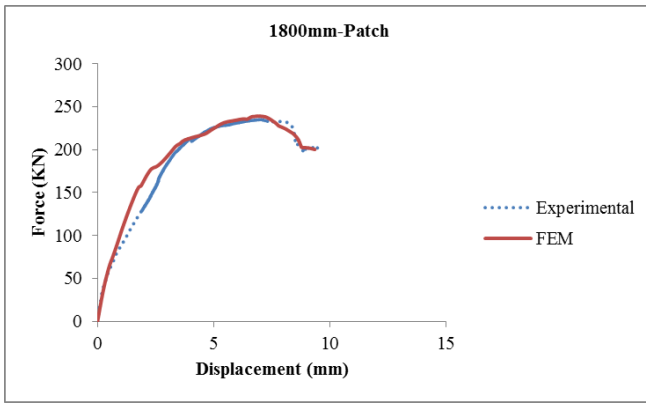
The figure 11 compares the load deflection curves for all the beams numerically analyzed in this study. It can be seen that cracking for all beams initiated at nearly the same load as discussed in section 4.1 but at different load increments
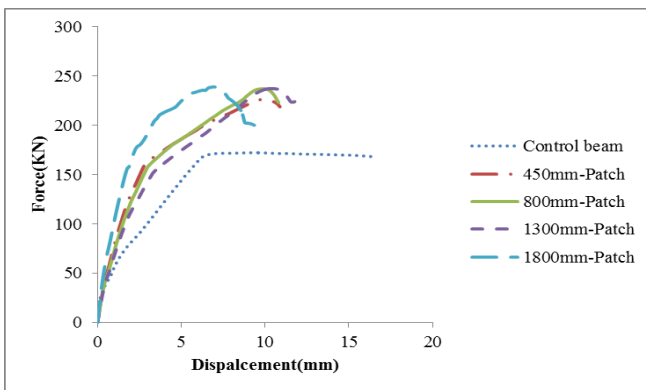

Figure 11: Load deflection curves for all beams analyzed [26]

This means that the effect of patch repair was to delay crack initiation. For beams repaired over a length of 450mm, 800mm and1300mm the behavior was more or less the same except the differences in yielding and debonding which occurred at different loads and displacement. Beam with 1800mm length patch repair showed a slightly different load displacement relationship. In comparison with the behavior of other beams, the behavior is relatively brittle since the debonding load was high but at small deflection as compared to other beams. The reason may probably be attributed to the reduction in tension steel cross section and large size of repair with high tensile strength.

4.3. Damage energy release rate.

Damage energy release rate is another parameter that can be used to study the overall behavior of reinforced concrete beams under bending. In fact, the four stages of failure, i.e. cracking initiation, yielding of steel, debonding load for strengthened beams and crushing load may be readily identified on the load-energy relationship, as it is seen in Figure 12. This is the energy dissipated when concrete is undergoing damage failure. From the figure, it can be observed that after yielding, the energy release rate is highly nonlinear indicating extensive deformation (cracking) of different reinforced concrete beams. The output in terms of load versus energy from Abaqus clearly shows that concrete starts to release energy after a number of load increments, and that before cracking the energy release rate is zero and then starts to increase linearly up to yielding.
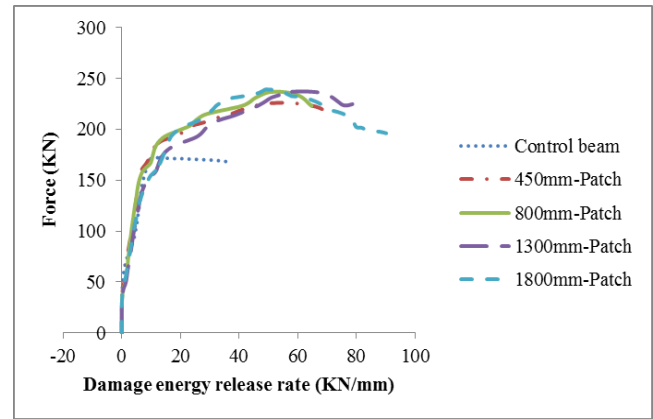
4.4. Strain distribution in FRP

Debonding of FRP plate from concrete is a special failure mode associated with strengthened RC beams. It is caused by high interfacial stress concentrations around flexural or flexural-shear cracks or at the plate end. A common measure used to control debonding is to limit the strain in the FRP material to a usable or debonding strain which, when exceeded at some locations, FRP will separates from the beam. Strain in FRP is mostly a governing factor in design of strengthened RC beams. The figure 13 shows the strain distribution for analyzed beams from where it is observed that as the length of the patch is becoming larger, strain distribution was becomes uniform. This shows that the discontinuity in the material to which FRP is bonded affects the strain distribution in FRP which in turns affect the debonding failure. It is clear that there is a peak strain in FRP at which debonding is initiated.

[2] recommends that in order to prevent debonding of the FRP laminate, a limitation should be placed on the strain level developed in the laminate. ACI proposed the following expression for debonding or usable strain:

$$\varepsilon_{fd} = \kappa_m \varepsilon_{fu} \qquad (7)$$

where ε_{fu} is the design rupture strain given by the manufacturer as 1.7% and κ_m is the bond dependent coefficient given by

$$\kappa_m =$$

$$\begin{cases} \dfrac{1}{60\varepsilon_{fu}}\left(1 - \dfrac{nE_f t_f}{360000}\right) \leq 0.90 \ for \ nE_f t_f \leq 180000 \\ \dfrac{1}{60\varepsilon_{fu}}\left(\dfrac{90000}{nE_f t_f}\right) \leq 0.90 \ for \ nE_f t_f \prec 180000 \end{cases}$$

(8)

where E_f is the tensile modulus of elasticity of FRP (MPa), t_f is the nominal thickness of one ply of FRP reinforcement in mm, ε_{fu} is the design rupture strain of FRP in mm/mm and n is the number of plies used.

Figure 13: Strain distribution in FRP

Figure 13. Intermediate crack induced debonding
(a)

Figure 13. Intermediate crack induced debonding
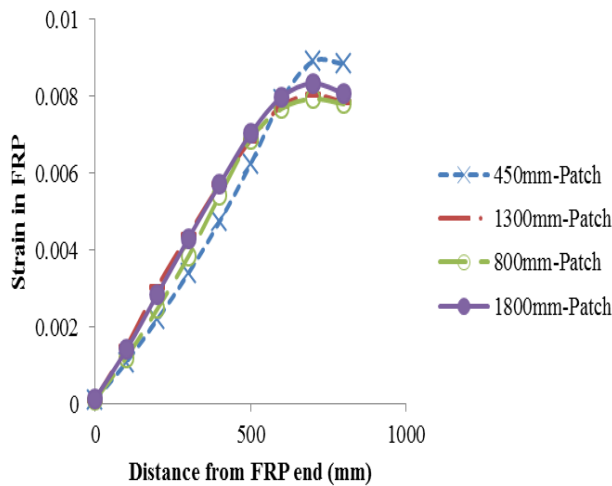(b)

The table 1 compares the peak strain from our finite elements analysis with ACI prediction. It is clear that there is a good agreement between the two, hence the integrity of our model. From our finite elements analysis, the peak strain in FRP was in the constant bending moment or just under loading points. That is where debonding initiated.

The Table about Comparison of debonding strain: FEM vs ACI 440.2R-02is presented bellow.

Table 1: Comparison of debonding strain: FEM vs ACI 440.2R-02.

Beam type	FEM*	ACI 440.2R-02**	% difference
450mm-Patched beam	0.00792	0.00765	3.4
800mm-Patched beam	0.00768	0.00765	0.4
1300mm-Patched beam	0.00775	0.00765	1.3
1800mm-Patched beam	0.00799	0.00765	4.3

*Finite Elements Method, the numerical analysis method used here
**American Concrete Institute recommendations, 2002.

This is also in accordance with findings of [23] which stipulates that ACI accurately predicts strain in FRP for relatively long laminates and for steel reinforcement ratios that exceeds 0.35%.

4.5. Failure mechanism
As discussed in section 4.4 maximum debonding strain in FRP was in the constant bending moment region or just under loading points and debonding initiated at those locations. Thus, the failure mode was intermediate crack induced debonding followed by concrete crushing. This is shown by Figure 13.
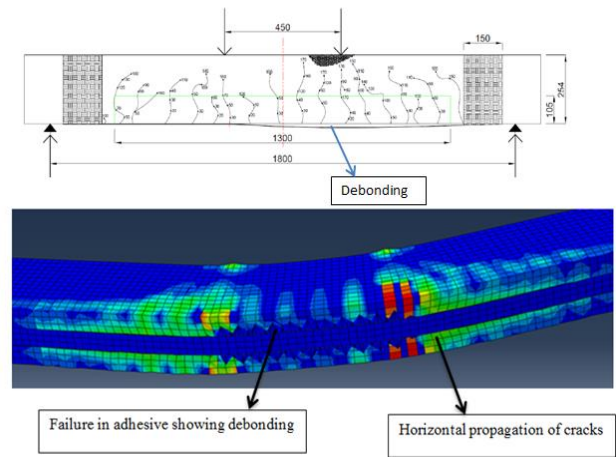
V. CONCLUSION

In this study, a finite element model was developed for analysis of reinforced concrete beams patch repaired and strengthened with FRP composites by varying the length of the patch. Concrete damaged plasticity model was used for the behavior of both concrete and repair material; linear elastic-perfectly plastic model for steel; cohesive zone model for the interface between concrete and FRP and elastic isotropic model for CFRP.

Results from finite elements analysis were in good agreement with experimental findings in terms of load deflection relationships, failure mechanism and structural crack distribution. Cracking loads were accurately found from damage energy release rate. Also strain distribution in FRP from the present analysis was in good agreement with ACI recommendation about the limiting strain or debonding strain in FRP. The study confirmed the possibility and importance of structural strengthening of deficient structures, as it increases the load carrying capacity as long as the overall level of performance of the concerned structure is still acceptable.

The results from this study clearly show the ability of the proposed model for analyzing the overall behavior of patch-repaired beams and strengthened with FRP composites. Despite these good results, future researches should continue putting much effort in the energy approaches to study the behavior of patch repaired and strengthened reinforced concrete beams particularly the debonding failure.

Finite Element Modeling of Reinforced Concrete Beam Patch Repaired and Strengthened with Fiber-Reinforced Polymers

REFERENCES

[1] Abaqus/CAE User's Manual, 2010.

[2] American Concrete Institute. Guide for the design and construction of externally bonded FRP systems for strengthening concrete structures. ACI 440.02R, Detroit.

[3] Au, C. & Buyukozturk, O. 2006. Debonding of FRP plated concrete: A tri-layer fracture treatment. Engineering Fracture Mechanics. 73(3):348-365.

[4] Baky, H.A., Ebead, U.A. & Neale, K.W. 2007. Flexural and interfacial behavior of FRP-strengthened reinforced concrete beams. Journal of Composites for Construction. 11(6):629-639.

[5] Buyukozturk, O. 1976. Nonlinear analysis of reinforced concrete structures. Journal of Composites and Structures. 7: 149-156.

[6] Camata, G., Spacone,E. & Zarnic, R. 2007.Experimental and nonlinear finite element studies of RC beams strengthened with FRP plates. Journal of Composites: Part B. 38: 277-288.

[7] Chaudhari, S.V & Chakrabarti, M.A. 2012. Modeling of concrete for nonlinear analysis using finite element code ABAQUS. International Journal of Computer Applications. 44 (7): 14-18.

[8] Chen, G.M., Teng, J.G., Chen, J.F & Rosenboom, O.A. 2008. Finite element model for intermediate crack debonding in RC beams strengthened with externally bonded FRP reinforcement. Proceedings of the fourth International Conference on FRP Composites in Civil Engineering. 22-24 July 2008, Zurich, Switzerland.

[9] Eurocode 2. 2004. Design of concrete structures. Part 1-1: General rules and rules for buildings.

[10] Hearing, B.P. 2000. Delamination in Reinforced Concrete Retrofitted with Fiber Reinforced Plastics. Ph.D disseltation, Department of Civil and Environmental Engineering, Massachusetts Institute of Technology, Cambridge, Massachusetts.

[11] Hillerborg, A., Modéer, M. & Petersson, P-E. 1976. Analysis of crack formation and crack growth in concrete by means of fracture mechanics and finite elements. Journal of Cement and Concrete Research. 6: 773-782.

[12] Kwak, H-G & Filippou, F.C. 1990. Finite element analysis of reinforced concrete structures under monotonic loads. (Report N0 UCB/SEMM-90/14). University of California: Structural Engineering, Mechanics and Materials.

[13] Lubliner, J., Oliver, J., Oller, S. & Onate, E. 1989. A plastic damage model for concrete. International Journal of Solids and Structures. 25(3): 299-326.

[14] Malek, A.M., Saadatmanesh, H. & Mohammad, R.E. 1998. Prediction of Failure Load of R/C Beams Strengthened with FRP Plate Due to Stress Concentration at the Plate End. ACI Structural Journal. 95(1):142-152.

[15] Malumbela, G. 2010. Measurable parameters for performance of corroded and repaired RC beams under load. PhD Thesis. University of Cape Town.

[16] Mattys, S. 2000. Structural behavior and design of concrete members strengthened with externally bonded FRP reinforcement. PhD Thesis. Ghent University.

[17] MUNDELI, S. 2014. Behavior of RC Beams Patch Repaired and Strengthened with FRP Composites. Msc Thesis. University of Cape Town.

[18] Obaidat, Y.T., Heyden, S. & Dahlblom, O. 2010. The effect of CFRP and CFRP/concrete interface models when modeling retrofitted RC beams with FEM. Journal of Composites Structures. 92: 1391-1398.

[19] Rabinovitch, O. & Frostig, Y. 2001. Delamination Failure of RC Beams Strengthened with FRP Strips-A Closed -Form -High Order and Fracture Mechanics Approach. Journal of Engineering Mechanics. 127(8):852-861.

[20] Rio, O., Andrade, C., Izquierdo, D. & Alonso, C. 2005. Behavior of Patch-repaired concrete structural elements under increasing static loads to flexural failure. Journal of Materials in Civil Engineering. 17(2): 168-177.

[21] Simonelli, G. 2005. Finite element analysis of RC beams retrofitted with fibre reinforced polymers. PhD Thesis. Università degli Studi di Napoli Federico II, London.

[22] Smith, S.T. & Teng, J.G. 2001. Interfacial stresses in plated beams. [Engineering Structures]. 23(7):857-877.

[23] Supaviriyakit, T. Pornpongsaro, P. & Pimanmas, A. 2004. Finite element analysis of FRP-strengthened RC beams. Songklanakarin J. Sci. Technol. 26 (4): 497-507.

[24] Täljsten, B. 1996. Strengthening of concrete prisms using the plate-bonding technique. International Journal of Fracture. 82:253-266.

[25] Teng, J.G. & Chen, J.F. 2009. Mechanics of debonding in FRP-plated RC beams. Proceedings of the Institution of Civil Engineers, Structures and Buildings. 162(SB5):335-345.

[26] Tounsi, A. and others. 2009. Interfacial stresses in FRP-plated RC beams: effect of adhered shear deformations. International Journal of Adhesion and Adhesives. 29(4):343-351.